PROTEINS
STRUCTURE ■ FUNCTION ■ BIOINFORMATICS

Analysis of electrostatic contributions to the selectivity of interactions between RING-finger domains and ubiquitin-conjugating enzymes

Johanna Scheper,[1] Baldo Oliva,[2] Jordi Villà-Freixa,[2]* and Timothy M. Thomson[1]*

[1] Department of Molecular and Cell Biology, Instituto de Biología Molecular de Barcelona, Consejo Superior de Investigaciones Científicas, Barcelona, Spain

[2] Research Group on Biomedical Informatics, Departament de Ciències Experimentals i de la Salut, Institut Municipal d'Investigació Mèdica, Universitat Pompeu Fabra, Barcelona, Spain

ABSTRACT

The zinc-coordinated protein motifs known as RING-finger domains, present on a class of ubiquitin ligases (E3's), recruit ubiquitin-conjugating enzymes (E2s), tethering them to substrate proteins for covalent modification with ubiquitin. Each RING-finger domain can recruit different E2s, and these interactions are frequently selective, in that certain RING-finger domains associate preferentially with certain E2s. This selectivity acquires particular biological relevance when the recruited E2s exert specialized functions. We have explored the determinants that specify the presence or absence of experimentally detectable interaction between two RING-finger domains, those on RNF11 and RNF103, and two E2s, UBC13, a specialized E2 that catalyzes ubiquitin chain elongation through Lys63 of ubiquitin, and UbcH7, which mediates polyubiquitylation through Lys48. Through the iterative use of computational predictive tools and experimental validations, we have found that these interactions and their selectivity are partly governed by the combinations of electrostatic interactions linking specific residues of the contact interfaces. Our analysis also predicts that the main determinants of selectivity of these interactions reside on the RING-finger domains, rather than on the E2s. The application of some of these rules of interaction selectivity has permitted us to experimentally manipulate the selectivity of interaction of the RING-finger domain-E2 pairs under study.

Proteins 2009; 74:92–103.

Key words: protein interactions; RING-finger domains; ubiquitin-conjugating enzymes; free energy calculations; homology modeling; electrostatic interactions.

INTRODUCTION

Many biochemical processes are governed by interactions between macromolecules, including recognition between proteins through specialized modules. Each class of interaction modules is usually present in different versions in a given organism, and these differences confer each particular module with the capacity to engage in selective or preferential interactions, usually defined by higher binding affinities between the interacting partners.[1,2] A second mechanism that determines interaction selectivity is based on modulation of the structure or the binding properties of the interaction partners by phosphorylation, acetylation, or other covalent modifications. Third, selectivity can be dictated by noncovalent steric modulation such as in co-operative interactions. A fourth mechanism, accessibility based on differential coexpression or subcellular localization, also called contextual specificity, is not governed by intrinsic properties of the interacting partners.[1] The selectivity of interactions between proteins and other macromolecules is a fundamental premise for the directionality and effective function of all biochemical networks, reducing entropy to levels that permit the occurrence of life.

Protein–protein interactions can be classified into two broad categories, recognition of short peptides and binding through interaction patches. Interactions of the first category have been thoroughly studied, and selectivity rules for preferential peptide recognition have been deduced for several recognition modules, exemplified by SH2, FHA, SH3, WW, or PDZ motifs.[3–9] The overall conclusion from these studies is that several consensus residues on the binding peptides are essential for recognition by all members of a class of recognition modules, and that residues outside this essential core confer

Additional Supporting Information may be found in the online version of this article.

Grant sponsor: Spanish Ministry of Education; Grant numbers: SAF2005-05109-CO2-01, BIO2005-00533, PROFIT PSE-010000-2007-1; Grant sponsor: QosCosGrid STREP Project; Grant number: BQU2003-0448.

*Correspondence to: Timothy M. Thomson or Jordi Villà-Freixa. E-mail: titbmc@cid.csic.es or jvilla@imim.es

Received 15 January 2008; Revised 28 March 2008; Accepted 14 April 2008
Published online 9 July 2008 in Wiley InterScience (www.interscience.wiley.com).
DOI: 10.1002/prot.22120

selectivity properties, by which a specific peptide will be preferentially recognized by specific subsets of the recognition modules.[1,2] Reciprocally, specific peptide recognition modules preferentially interact with specific subsets of their cognate peptide families. Despite the inference of selectivity rules that allow relatively good predictions of specific protein–protein interactions, experimental verification by several *in vitro* methods shows that there can be substantial overlaps in interaction preferences between different peptides and recognition modules, which raises the question of how this apparent *in vitro* promiscuity translates into *in vivo* selectivity. Regarding this, a number of studies suggest that cell-based binding assays, such as yeast two-hybrid, might be more reliable indicators of the *in vivo* interaction selectivities of protein recognition domains than affinity determinations of purified proteins in purely *in vitro* assays.[1,10]

Protein–protein interactions that use larger surfaces or patches for mutual recognition follow more complex rules to achieve interaction selectivity, because several regions on each interface contribute to the overall affinity and specificity of interaction, through co-operative or antagonistic effects.[11] This complexity has had a deterrent effect on the systematic study of the rules that govern the selectivity of this class of interactions.

RING-finger domains are loop-helix-loop structures that contain eight conserved histidine and cysteine residues that coordinate two central Zn^{2+} ions in a cross-brace organization.[12] These domains engage in interactions with the Ubc domains of ubiquitin-conjugating enzymes (or E2s) and thus serve to tether the latter to complexes dedicated to the covalent modification of substrate proteins by ubiquitin. Therefore, although they can interact with other protein modules, RING-finger domains define most proteins as ubiquitin ligases, also known as E3s.[13] Over 500 human proteins bear RING-finger domains, thus constituting the largest class of functionally related proteins.[14] The E2s recruited by these proteins can exert diverse functions, including the transfer of a single ubiquitin moiety to substrate proteins (monoubiquitylation), the elongation of polyubiquitin chains through the catalysis of thioester bond formation based on Lys 48 of ubiquitin (sometimes called canonical polyubiquitylation), polyubiquitylation through Lys 63 (or lysines at other positions) of ubiquitin, or the conjugation to substrate proteins of ubiquitinlike proteins such as SUMO (sumoylation) or Nedd8 (neddylation).[13] Therefore, the recruitment by RING-finger domains of a particular E2 will determine the specific modification to which substrate proteins are subjected, which will determine the eventual fate of the modified protein. The prediction of such specific activities of proteins bearing RING-finger domains requires a knowledge of which of the functionally diverse E2s can be selectively recruited by a particular RING-finger domain. We have approached this issue by a comparative analysis of the interactions between two E2s, Ubc13 and UbcH7, and two RING-finger domains with different relative selectivities, the more selective domain from RNF11, and the more promiscuous domain from RNF103.

RESULTS

RING-finger domains with different selectivity for interaction with E2s

Prior work in our laboratory aimed at identifying interactors of the ubiquitin-conjugating enzyme Ubc13 yielded seven different interactors.[15] With the exception of the Ubc13 heterodimerization partners UEV1 and UEV2, all Ubc13 interactors contain a RING-finger domain, which was required for these interactions.[15] The specificity of interaction between these RING-finger domains with Ubc13 and other E2s was also tested by yeast two-hybrid assays, which showed that, except for the RING-finger domain on RNF11, all other Ubc13 interactors also interact with other E2s.[15] Figure 1 shows additional examples of selective interactions between the RING-finger domain proteins RNF11, RNF103, and ZFRF2 with the E2s Ubc13 and UbcH7.

These experiments show, not unexpectedly, that a given E2 can interact with multiple RING-finger domains and, conversely, that a given RING-finger domain has the capacity to interact with more than one E2.[15,16] They also show that there is a selectivity in the recruitment of different E2s by different RING-finger domains. The recruitment of Ubc13 and other E2s to the RING-finger domains studied here implies that the same E3 can function as a ligase in more than one class of polyubiquitylation, and therefore the specific E2 recruitment determines the function of the E3 in the final fates of the modified substrate proteins.

Molecular modeling of the RING-finger domains from RNF11 and RNF103

RING-finger domains can have widely divergent sequences in the intervening loops between the metal-coordinating Cys and His, and yet recruit very similar sets of E2s.[17] As shown for other protein recognition modules,[10,18,19] alignments of primary sequences were poor predictors of the selectivity of interaction between RING-finger domains and E2s (Supplementary Material). We reasoned that a structure-based analysis could provide us with better insights regarding this.

The crystal structures of both Ubc13 and UbcH7 are available.[20,21] Relevant to our approach, the crystal structure of UbcH7 has been resolved in complex with the RING-finger domain of c-Cbl.[21] To model the complexes between the two RING-finger domains and the two E2s of interest, a substitution strategy was used, in which models were first generated for the RING-finger proteins of

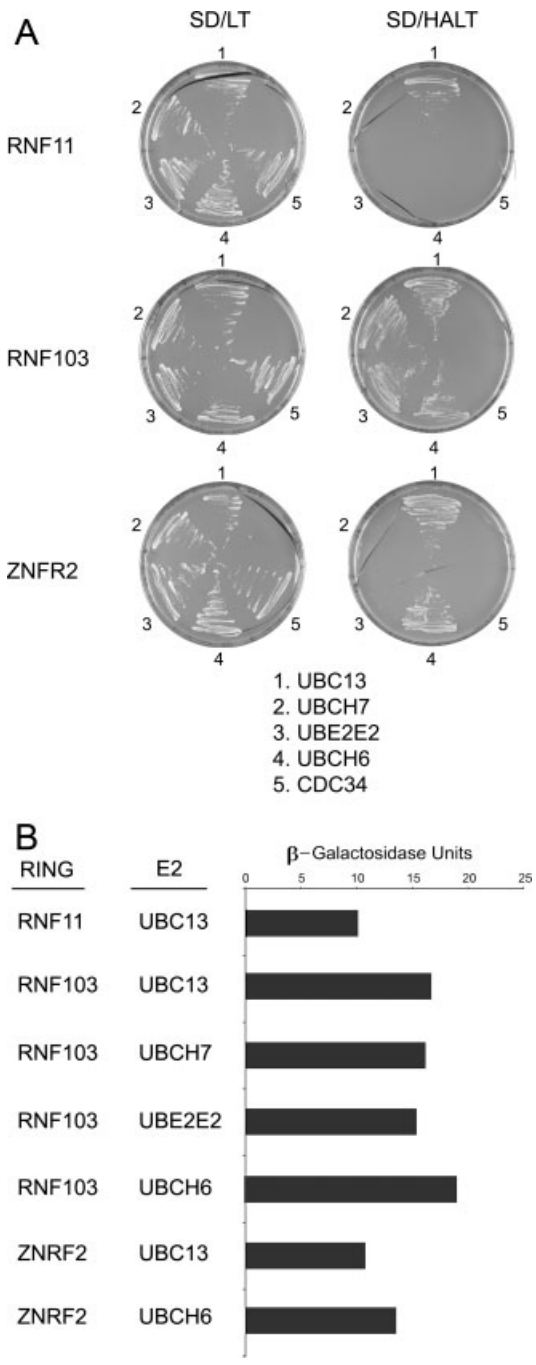

Figure 1

Selective interactions between three RING finger proteins, RNF11, RNF103 and ZNFR2, with the ubiquitin-conjugating enzymes UBC13, UBCH7, UBE2E2, UBCH6 and CDC34, as determined by yeast two-hybrid assays. (**A**) Growth of AH109 strain yeast cells transformed with pairwise RING finger - UBC combinations and plated on SD/LT (Leu^-Trp^-) control medium, or SD/HALT ($His^-Ala^-Leu^-Trp^-$) quadruple selection medium. (**B**) Quantitation of β-galactosidase activity as a measure of strength of interaction between the indicated RING finger proteins and ubiquitin conjugating enzymes. Liquid cultures of yeast cells bearing the indicated interacting RING finger proteins and ubiquitin-conjugating enzymes, grown in quadruple-selection liquid medium, were assayed for their β-galactosidase activity.

RNF11 and RNF103 using the structure of equine herpes virus C3HC4 as the template and then superimposed upon the structure of c-Cbl within the c-Cbl-UbcH7 complex. For complexes in which the modeled RING-finger domains interact with UbcH7, the coordinates of the latter were maintained. For complexes with Ubc13, the models for the complexes were also obtained by substituting coordinates for UbcH7. The best models of heterodimers between E2s and RING-finger domains were chosen for our analysis on the basis of statistical potentials, exclusion of models with energy maxima, and visual inspection (Supplemental Figs. 2 and 3). It should be noted that the complex modeled between RNF11 and UbcH7 is not observed by yeast two-hybrid assays. We call these "non-productive" interactions, as opposed to those that we have verified experimentally by yeast two-hybrid assays, which we call "productive" interactions.

Inspection of the modeled complexes formed by RNF11 with either Ubc13 or UbcH7 (Figs. 2–4) provides several possible clues as to why the RNF11-Ubc13 interaction is readily detected experimentally, while the RNF11-UbcH7 interaction is unlikely to occur. First, in the productive RNF11-Ubc13 complex (see Fig. 3), M64 of Ubc13 fits well into the hydrophobic pocket formed by W129 and F134 of RNF11, and W95 of Ubc13 itself. On the left and central regions of the Ubc13 interphase, K10 and R7 have favorable electrostatic interactions with D105 and E98 of RNF11, respectively, contributing to the stability of the heterodimer. In contrast, in the nonproductive RNF11-UbcH7 complex, the same residues in RNF11 that provide a favorable environment for interaction with M64 in Ubc13, W129 and F134, hinder its interaction with UbcH7, which has a phenylalanine residue at the position equivalent to M64 of Ubc13 (see Fig. 4). This might be a relevant factor that prevents a productive interaction between these two proteins, overrunning other factors that might potentially favor a productive interaction, such as the electrostatic interactions between K122 of UbcH7 and E98 of RNF11, or between R6 of UbcH7 and D105 of RNF11 (Fig. 4).

In the model for the productive RNF103-Ubc13 complex, W651 in RNF103 makes favorable contact with M64 in Ubc13. This interaction is further stabilized by the favorable environment provided by W95 in Ubc13. Furthermore, the interface is stabilized by additional electrostatic interactions at either end, such as E620 in RNF103 with K10 in Ubc13 (see Fig. 5). In the RNF103-UbcH7 complex (see Fig. 6), also a productive interaction, W651 in RNF103 does not clash sterically with F63 of UbcH7, because the entire loop that contains this residue swings in such a way that F63 now fits into a pocket on RNF103 formed by E620 and W651. Furthermore, this positioning of RNF103 with respect to UbcH7 predicts the formation of π bonds between F63 in UbcH7 and W651 in RNF103, contributing to the stabilization of the complex (see Fig. 6).

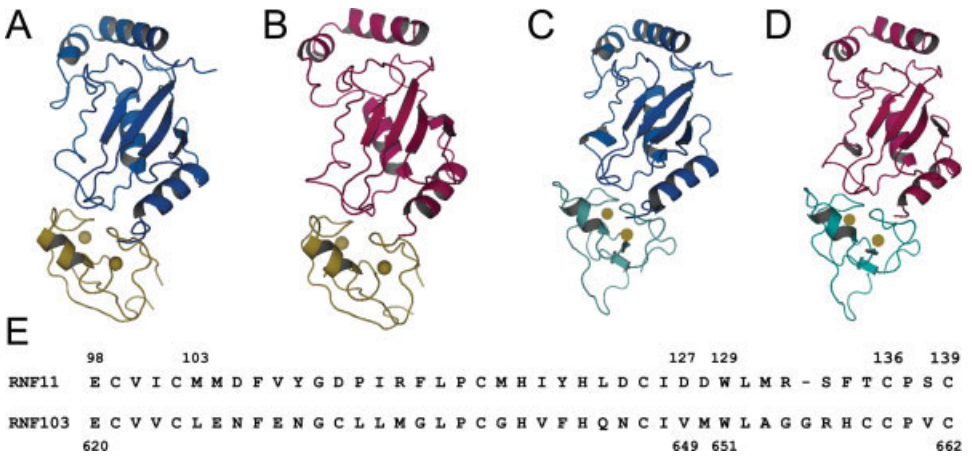

Figure 2

Models of pairwise complexes between the RING finger domains of RNF11 and RNF103 and the E2's Ubc13 and UbcH7. (**A**) RNF11-UBC13. (**B**) RNF11-UBCH7. (**C**) RNF103-UBC13. (**D**) RNF103-UBCH7. The Cys- and His- coordinated Zn^{2+} atoms are represented as spheres associated with the two RING finger domains. (**E**) Aligment of the RING finger domains of RNF11 and RNF103, indicating the positions of some of the most relevant residues discussed in the text. [Color figure can be viewed in the online issue, which is available at www.interscience.wiley.com.]

Second, the RNF11-UbcH7 interaction may be hampered by the position of M103 in RNF11 with respect to the UbcH7 interface (see Fig. 4). In the model, this residue protrudes from the surface of RNF11 toward a cleft placed between helix 1 and residue K122 of UbcH7. Although generated as a relaxed and minimized model, this configuration is predicted to be inherently unstable, because of the described potential steric constraints.

A point mutation at M103 in RNF11 causes less selective E2 recruitment

Several predictions emerge from the above-mentioned models: first, substitution of M64 in Ubc13 for a more bulky or more hydrophobic residue may prevent interaction with RNF11, and, conversely, substitution of F63 in UbcH7 for a less bulky or less hydrophobic residue may favor a productive interaction with RNF11. Alternatively, substitutions of residues at either end of the interface in UbcH7, RNF11, or both that allow loop sliding and accommodation of F63 in UbcH7 may favor interaction.

An additional prediction from the models is that the poor fitting of M103 in RNF11 onto residues in the middle loop and first helix of UbcH7 (see Fig. 4) could contribute to its failure to interact with RNF11 and therefore to the selectivity of recruitment of E2s by RNF11.

Several mutants were generated and experimentally tested for interaction. Contrary to our first set of predic-

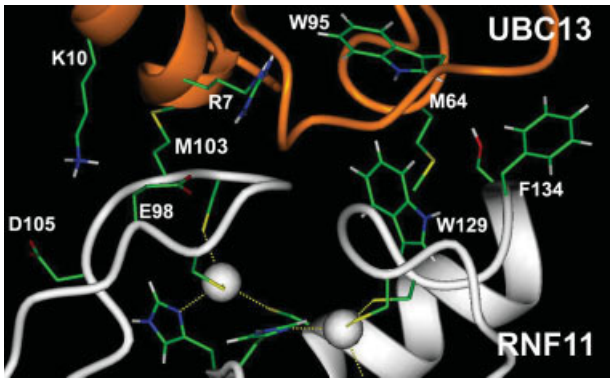

Figure 3

Interface of the modeled complex between the RING finger domain of RNF11 and Ubc13.

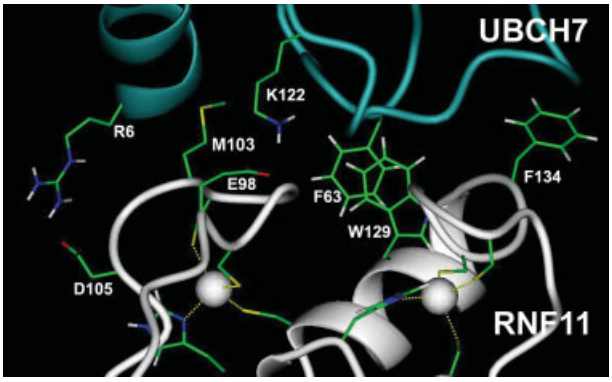

Figure 4

Interface of the modeled complex between the RING finger domain of RNF11 and UbcH7.

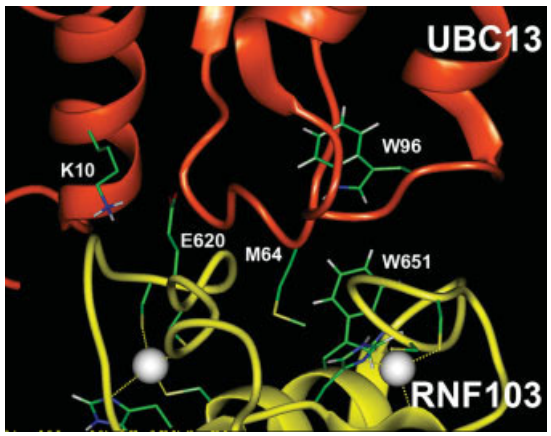

Figure 5

Interface of the modeled complex between the RING finger domain of RNF103 and Ubc13.

tions, the Ubc13^{M64F} mutant maintained its capacity to interact with both RNF11 and RNF103 in yeast two-hybrid assays (data not shown). On the other hand, mutation of F63 in UbcH7 to methionine (UbcH7^{F63M}) not only caused its interaction with RNF11, but also caused a loss of interaction with RNF103 (data not shown), therefore becoming more selective in its interaction with RING-finger domains. In conclusion, the presence of phenylalanine at position 63 in UbcH7 is not sufficient to explain by itself the selective interaction of UbcH7 with RNF103. Similarly, the presence of methionine at position 64 in Ubc13 does not explain by itself the more promiscuous RING-finger domain interactions of Ubc13.

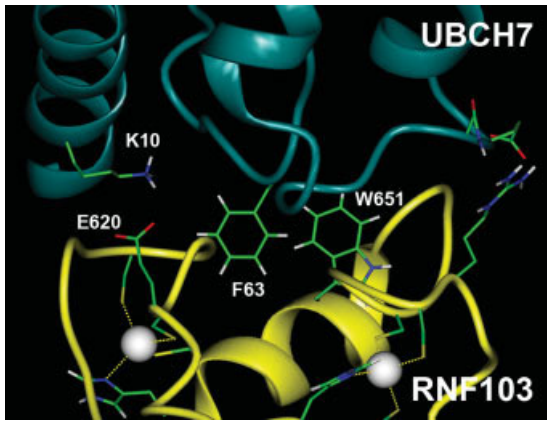

Figure 6

Interface of the modeled complex between the RING finger domain of RNF103 and UbcH7.

To experimentally test our second set of predictions, those implying M103 in RNF11 as a factor in E2 interaction selectivity, we generated substitutions at this position and assayed their interactions with Ubc13 and UbcH7 (see Fig. 7). Substitution of M103 for glycine or alanine (RNF11^{M103G} and RNF11^{M103A}) completely abolished the interaction of RNF11 with Ubc13, without gaining interaction with UbcH7 (see Fig. 7). Substitution for leucine (RNF11^{M103L}), a bulky hydrophobic residue, did not alter the interaction selectivity of wild-type RNF11, which continued to interact with Ubc13, but not with UbcH7 (see Fig. 7). Finally, substitution for valine (RNF11^{M103V}), a small hydrophobic residue, permitted the interaction of RNF11 with UbcH7, while maintaining its interaction with Ubc13 (see Fig. 7), thus effectively broadening its range of interactions with E2s.

These results indicate that a hydrophobic residue is required at position 103 for the interaction of RNF11 with both E2s. Thus, a strong dipole, such as a glycine residue, at this position, prevents the interaction of RNF11 with both E2s, even when the charge from this dipole is partially shielded, such as with an alanine substitution. They also show that a small hydrophobic residue, such as valine, at this position, in place of the sulphur-charged methionine, causes a loss of E2 interaction selectivity of RNF11. In conclusion, the selectivity of RING-finger-E2 interactions resides mostly on the RING-finger interactors. Specifically, both electrostatic and steric properties of residues at position 103 govern the E2 interaction selectivity of RNF11.

Additional electrostatic contributions to the stability and selectivity of the interactions between RING-finger domains and E2 proteins

The earlier results showed that the models were able to correctly predict some determinants of RING-finger-E2 interaction selectivity, but not others. To determine if

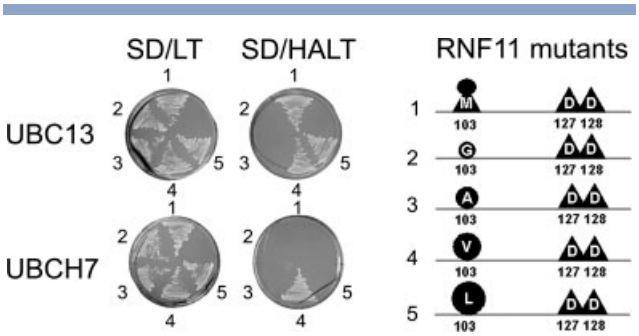

Figure 7

Interaction analysis between mutants at position 103 of RNF11 and the E2's UBC13 and UBCH7, determined by yeast two-hybrid assays. Yeast cells bearing constructs for the indicated RNF11 mutants and either UBC13 or UBCH7 were grown on plates with SD/LT control or SD/HALT quadruple selection medium.

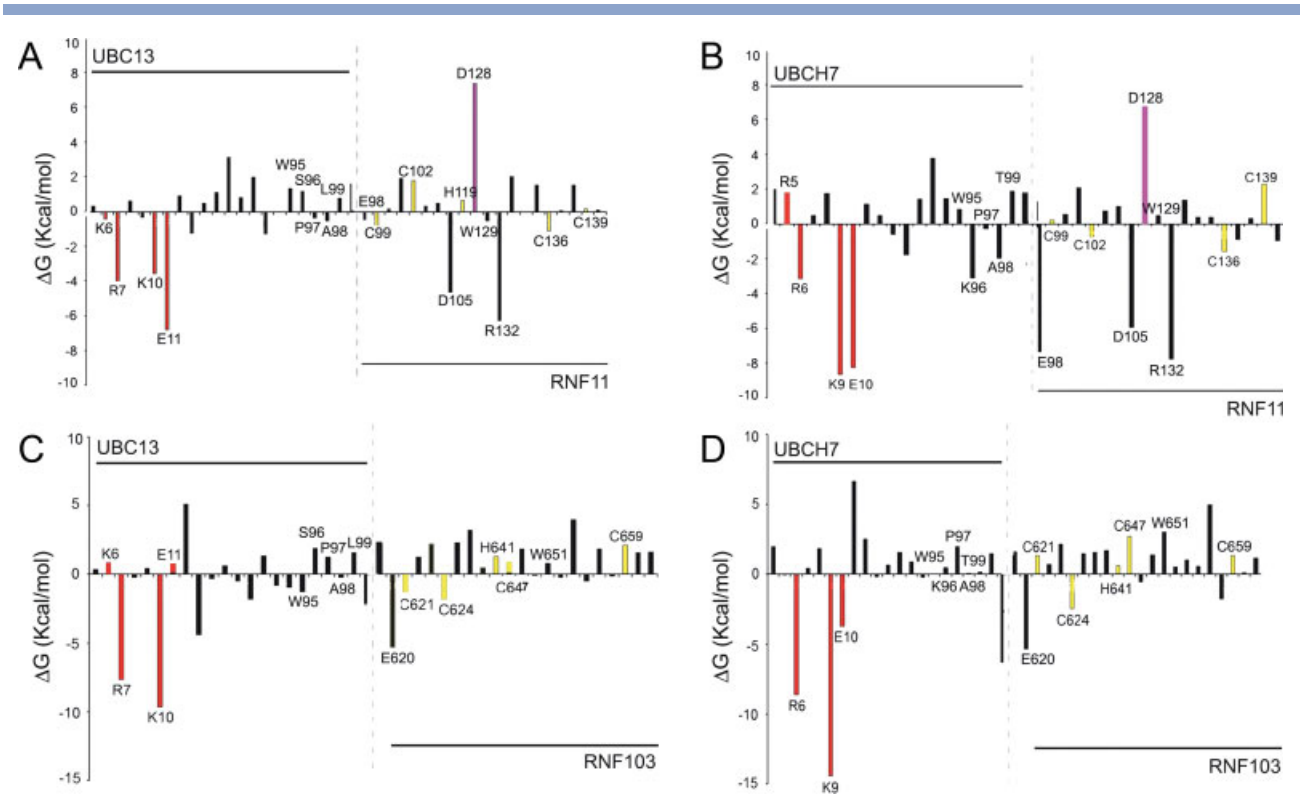

Figure 8

Electrostatic contributions to the stability of individual residues in the interfaces of the modeled complexes between the RING finger domain of RNF11 and Ubc13 (**A**), RNF11 and UbcH7 (**B**), RNF103 and Ubc13 (**C**), and RNF103 and UbcH7 (**D**). [Color figure can be viewed in the online issue, which is available at www.interscience.wiley.com.]

electrostatic contributions from additional regions in the RING-finger domains or the E2s under study could also play a role in RING-finger-E2 interaction selectivity, we conducted solvation free energy calculations of individual residues of interest with the PDLD/S-LRA method in the Molaris package.[21,22] For a variety of interaction modules, experimental and theoretical evidences suggest that nonpolar contributions are major contributors to interaction stability, while electrostatic contributions tend to specify interaction selectivity.[2,7]

We first estimated the contribution to the global free-binding energies of individual residues on the two interfaces in each of the modeled complexes (Fig. 8 and first columns of Supplementary Tables I–IV). In all four RING-finger domain-E2 complexes, one cluster of residues from the E2s was a major electrostatic contributor to the stability of the complexes. In Ubc13, this cluster was formed by R7, K10, and E11 in the interaction with RNF11, and by R7 and K10 in the interaction with RNF103 (see Fig. 8). In UbcH7, the cluster of polar residues formed by R6, K9, and E10 was the major contributor of the stability of interaction with both RNF11 and RNF103 (see Fig. 8).

The comparison of electrostatic energy contributions between residues in Ubc13 and residues in UbcH7 in their productive interactions with RNF103 showed few differences, as expected. Less expected was the occurrence of very few differences between Ubc13, which engages in a productive interaction with RNF11, and UbcH7, whose hypothetical interaction with RNF11 is nonproductive [Fig. 8(B)]. As described earlier, this might suggest once more that the strongest electrostatic determinants of selectivity may reside on the RING-finger domains, rather than on the E2-interaction partners.

We thus turned our attention to the electrostatic contributions to interaction stability of the residues in the RING-finger domains under study. On the RNF11 interface, D105 and R132 were strongly positive contributors ($\Delta G^{w\to p}_{PDLD/S,i} \ll 0$, where $\Delta G^{w\to p}_{PDLD/S,i}$ represents the difference in free energy of solvation between water and protein for a particular residue—see Methods section), and D128 was a strongly negative contributor ($\Delta G^{w\to p}_{PDLD/S,i} \gg 0$) both to the productive Ubc13-RNF11 interaction and to the nonproductive UbcH7-RNF11 interaction [Fig. 8(A,B)]. In the UbcH7-RNF11 model (which is nonproductive), a third strongly positive contributor to interaction stability, E98, was observed, this being a significant difference with the profile for the productive Ubc13-RNF11 interaction model [Fig. 8(B)].

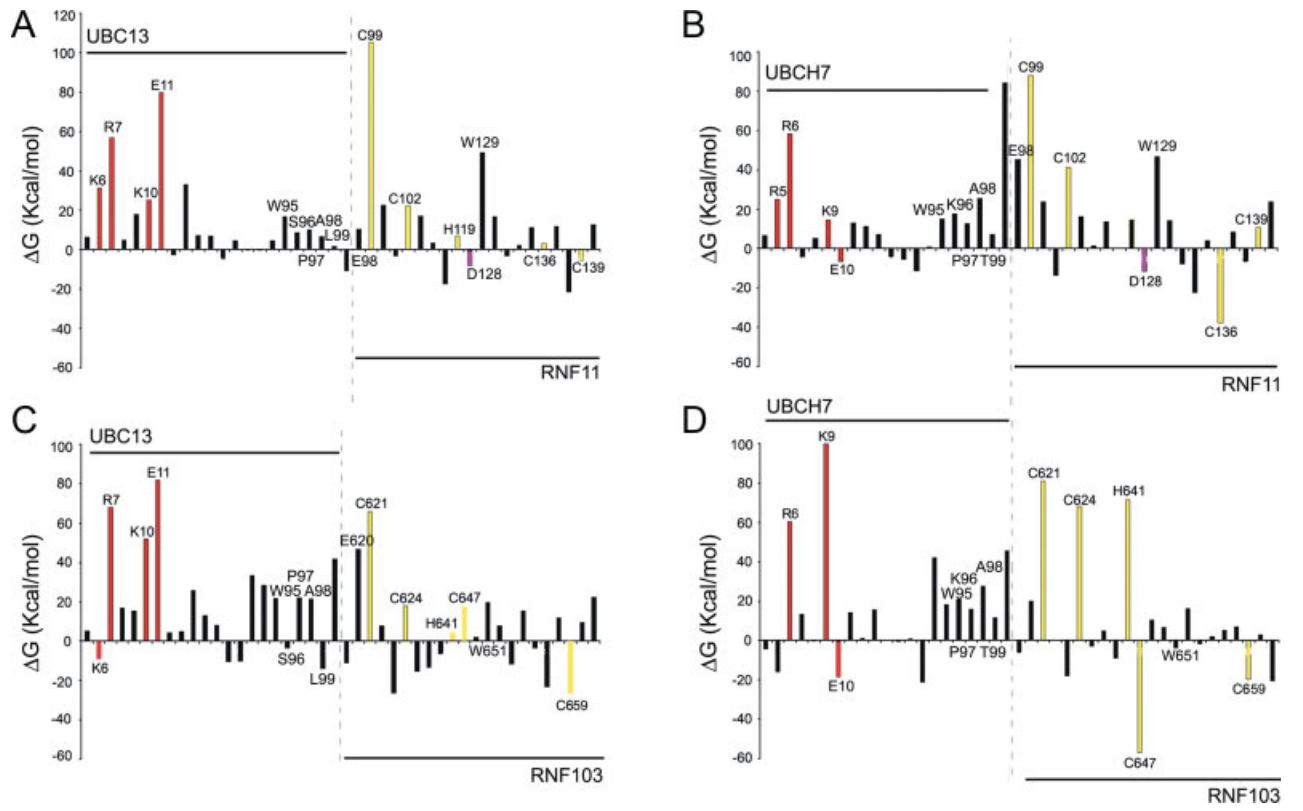

Figure 9

Effects of residue-wise virtual alanine mutagenesis (charge zeroing) on global free-binding energies (*S* in the Methods section) of the modeled complexes between the RING finger domain of RNF11 and Ubc13 (**A**), RNF11 and UbcH7 (**B**), RNF103 and Ubc13 (**C**), and RNF103 and UbcH7 (**D**). [Color figure can be viewed in the online issue, which is available at www.interscience.wiley.com.]

Compared to RNF11, the profile of residue-wise electrostatic contributions for RNF103, a promiscuous E2 interactor, is relatively flat, with the exception of E620, a strong positive contributor to the free binding energy in the RNF103-Ubc13 interaction [Fig. 8(C)]. This suggests that the electrostatic components contributed little to the stability of the RNF103 interactions or were even unfavorable for these interactions. E98 in RNF11 is equivalent to E620 in RNF103, which is predicted to favor the RNF103-UbcH7 interaction. Based on their electrostatic profiles, the prediction is that E98 should also favor the hypothetical interaction of RNF11 with UbcH7, which is nonproductive [Fig. 8(D)]. This seeming contradiction could be reconciled by making the assumption that the presence of three strongly positive contributors to the stability of the interaction between RNF11 and UbcH7 could confer excessive rigidity to the interface, preventing the loop swinging that may be required to accommodate F63 in UbcH7 onto the receiving hydrophobic groove on the surface of RNF11.

Virtual mutagenesis identifies residues that contribute to the selectivity of E2-RING-finger domain interactions

The earlier analysis predicted some of the key residues potentially contributing with their electrostatic interaction energies to the overall binding energy and stability of the modeled complexes and also some residues that may contribute to the selectivity of interaction of a given RING-finger domain. However, it could also mask the contribution of other residues, especially if they are located in the vicinity of the strongest binding energy contributors. To systematically predict the contribution of all possible residues (within 10 Å of the interface) to the interaction binding energy of a given E2-RING-finger domain pair, we performed a virtual mutagenesis approach, in which the electrostatic contribution of each residue, one at a time, was brought down to zero, followed by an estimation of the global free-binding energy of the system done by a simple summation of the $\Delta G^{w\to p}_{PDLD/S,i}$ of all residues (Fig. 9 and third column in

Supplementary Tables I–IV). Note that the overall summation is an extensive property, and as such it cannot be used to compare between different complexes just to estimate the qualitative contribution to binding of the charge-depleted residue. In this way, the perturbations in the stability of the system caused by the depletion of the charge contribution of each residue represent a measure of the contribution of that residue to the global stability of the interaction. This approach, which we call "charge zeroing," can be related to the alanine scanning in experimental mutagenesis and complements the profiles of electrostatic contributions of each residue to the RING-finger domain-E2 interactions, described earlier. The relationship between charge zeroing and computational alanine scanning is not precise as the latter would imply changes in van der Waals interactions that are neglected in the former. However, by neglecting such contributions, one emphasizes the long-range electrostatic properties of the protein–protein interface, while keeping the simulation protocol simple and tractable in a complete scanning of a portion of the sequence.

Charge zeroing of most residues on the E2 and RING-finger interfaces caused significant increases in the global electrostatics components of the free energy, indicating a destabilization of the interactions as shown in the qualitative estimates in Figure 9. This was clearly evident when zeroing the residues predicted from the binding energy calculations conducted earlier, K6, R7, K10, and E11 in Ubc13 and R5, R6, K9, and E10 in UbcH7 (Fig. 9 and Supplementary Tables I–IV). The charge depletion of these residues resulted in large increases in the global free-binding energies of the complexes and thus a profound destabilization of the complexes, confirming the strong contribution of these residues to the interactions as predicted from their electrostatic contribution profiles (see Fig. 8). Importantly, charge zeroing unveiled the contribution of residues that were not predicted from the previous calculations, or from the models, to play significant roles in the stability of the interactions, such as W95, S96, P97, A98, and L99 in Ubc13, and W95, K96, P97, A98, and T99 in UbcH7 (see Fig. 9). However, charge zeroing did not yield significant differences in electrostatic contribution profiles between E2s in productive (RNF11-Ubc13) and nonproductive (RNF11-UbcH7) complexes.

In contrast, this approach yielded significant differences in electrostatic contributions of equivalent residues between RING-finger domains that engage in productive (RNF103-UbcH7) and nonproductive (RNF11-UbcH7) interactions. Charge zeroing of the cysteine or histidine residues that participate in the coordination of Zn^{2+} atoms destabilized all complexes (see Fig. 9). One relevant exception was C136 in RNF11, whose charge zeroing did not affect significantly the stability of interaction with Ubc13 or UbcH7 (see Fig. 9). A second relevant exception was C139 in RNF11, whose zeroing stabilized the interaction with UbcH7, but not with Ubc13 (see Fig. 9), suggesting a negative contribution of this residue, or neighboring residues, to the UbcH7-RNF11 interaction.

As predicted from their electrostatic contribution profiles, charge zeroing of E620 in RNF103 and E98 in RNF11 caused a strong destabilization of their interactions with both Ubc13 and UbcH7 (see Fig. 9). These two residues contributed equally to productive and nonproductive interactions, and therefore they do not determine selectivity of interactions between the RING-finger domains and E2s studied here. An interesting situation was observed in the nonproductive UbcH7-RNF11 complex, in which charge zeroing of D128 in RNF11 caused a relative stabilization of the complex (see Fig. 9). The binding energy calculations had suggested that this residue plays a destabilizing role in the complex. Therefore, a prediction from these analyses is that the experimental substitution of D128 for a residue that is either relatively uncharged or with a positive charge might contribute to the stabilization of the interaction between RNF11 and UbcH7, and thus this residue and its surrounding region could be a determinant of selectivity in RING-finger-E2 interactions.

Point mutations at positions 649 or 650 in RNF103 cause more selective E2 recruitment

The earlier virtual analyses predicted that D128 in RNF11 or its surrounding region could contribute to its selective interaction with Ubc13. Therefore, the aspartates at positions 127 and 128 in RNF11 were substituted for leucine as a single mutant ($RNF11^{D128L}$), a double mutant ($RNF11^{D127LD128L}$), or a triple mutant in which M103 was also substituted for Leu ($RNF11^{M103LD127LD128L}$). All these mutants maintained their interaction with Ubc13, but did not gain interaction with UbcH7 (Fig. 11(A) and Supplementary Figure 4). Therefore, positions 127 and 128 in RNF11 do not contribute to the selectivity of interaction with different E2s.

The residues in RNF103 with positions equivalent to the strongly charged D127 and D128 in RNF11 are V649 and M650 [Fig. 8(A,B)]. The potential electrostatic contribution of these two residues to the stability of the UbcH7-RNF103 interaction was analyzed by estimating the global free-binding energies that result from substituting V649 and M650 for aspartate at both positions. The global free-binding energies were significantly increased in the substituted forms of UbcH7 (Fig. 10 and Supplementary Table V), suggesting that the hydrophobic nature of valine and methionine at these positions contributes to the stability of the complex, and possibly to the promiscuous recruitment of E2s by RNF103.

To test this hypothesis, methionine or valine residues were experimentally substituted for aspartate at positions 649, 650, or both, in RNF103 ($RNF103^{V649D}$, $RNF103^{M650D}$, and $RNF103^{V649DM650D}$). All these substitu-

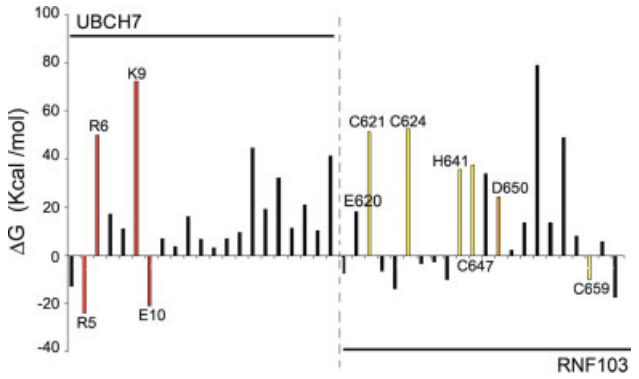

Figure 10

Effects of virtual mutagenesis of valine and methionine at positions 649 and 650 of RNF103 to aspartic acid on the global free-binding energies of the modeled complex between the RING finger domain of RNF103 and Ubc13. [Color figure can be viewed in the online issue, which is available at www.interscience.wiley.com.]

tions caused a loss of interaction of RNF103 with UbcH7, while maintaining its interaction with Ubc13 [Fig. 11(B) and Supplementary Fig. 4], thus confirming the importance of these residues for a promiscuous recruitment of E2s by RNF103. Therefore, substitutions with polar residues at positions 649 or 650 caused a more selective recruitment of E2s by RNF103.

On the other hand, having polar residues at equivalent positions in RNF11 do not prevent a more promiscuous recruitment of E2s. This is shown by the fact that the RNF11^{M103V} mutant described earlier, which contains two aspartates at positions 127 and 128 (equivalent to 649 and 650 on RNF103), interacted both with Ubc13 and UbcH7, which constitutes a loss of selectivity for the recruitment of E2s with respect to the wild-type RING finger (see Fig. 7). Reciprocally, RNF11 mutants bearing hydrophobic residues at positions 127–128 did not gain interaction with UbcH7 [Fig. 11(A)].

In conclusion, the presence of polar or hydrophobic residues at positions 127–128 in RNF11 or 649–650 in RNF103 can confer different selectivities of interaction with E2s depending on the context of the specific RING finger. More specifically, the presence of a small hydrophobic residue at position 103 in RNF11 favors a less selective recruitment of E2s by this RING-finger domain both with polar and hydrophobic residues at positions 127–128, while the presence of polar residues at positions 649–650 in RNF103 caused a more selective E2 recruitment.

DISCUSSION

We have used here a case-study approach to analyze some of the factors that determine the selectivity of interaction between RING-finger domains and E2s, in which we have compared a relatively selective E2 recruiter, RNF11, and a more promiscuous interactor, RNF103, in their ability to interact with two E2s, Ubc13 and UbcH7. We have applied three computational approaches, namely (1) molecular modeling of productive and nonproductive RING-finger domain-E2 complexes, (2) residue-wise calculation of electrostatic contributions to the stability of the complexes, estimated as relative-free energies of solvation of those residues with respect to water, and (3) virtual mutagenesis of the electrostatic contributions of each residue in the interfaces of such complexes. A general conclusion that we have drawn from these approaches is that the selectivity of interaction resides mainly on the RING-finger domains, and not on the E2s, at least in the pairwise complexes under study. This conclusion is a step forward compared to prior attempts to infer general rules of determinants of specificity of interaction between members of these two protein domain families.[23]

In addition to reaching this general conclusion, the application of several predictions from the molecular modeling and dynamics analyses and experimental verifications allowed us to create a RNF11 variant capable of interacting with UbcH7, thus effectively switching a selective RING finger to a more promiscuous E2 interactor by virtue of a single-point mutation (methionine for valine at position 103). Reciprocally, we turned a promis-

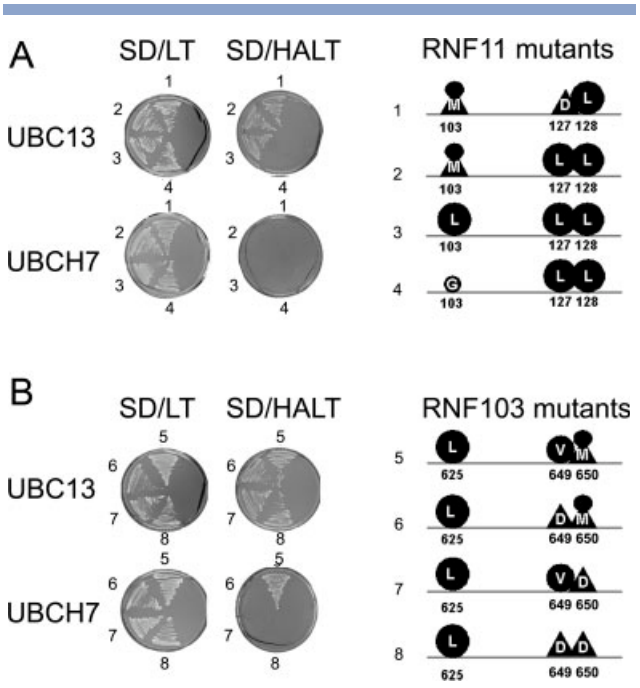

Figure 11

Yeast two-hybrid interaction analysis between mutants at positions 127 or 128 of RNF11 (**A**) and mutants at positions 649 or 650 of RNF103 (**B**) with UBC13 or UBCH7. Yeast cells bearing constructs for the indicated mutants and either UBC13 or UBCH7 were grown on plates with SD/LT control or SD/HALT quadruple selection medium.

cuous E2 interactor, RNF103, into a more selective one by mutating a single residue (valine for aspartic acid at position 649, or methionine for aspartic acid at position 650). These observations suggest that the presence of a hydrophobic residue at positions equivalent to 103 in RNF11 may favor the recruitment of a broader range of E2s. Also, RING-finger domains with polar residues at positions equivalent to D127 and D128 in RNF11 may be predicted to be more selective in their recruitment of E2s, and reciprocally, the presence of nonpolar residues at these positions, as in the case of RNF103, would be predictive of a more promiscuous recruitment of E2s. Therefore, at least two regions on the RING-finger domain interface contribute to their selective interactions with different E2s. A summary of the interactions, experimentally validated by yeast two-hybrid assays, between all RNF11 and RNF103 mutants with Ubc13 or UbcH7 is shown in Supplementary Figure 5.

Our computational analyses have yielded additional reasonably good predictions on the relevance of regions or individual residues to the stability of the two pairs of RING-finger domain-E2 complexes under study, without contributing to the selectivity of these interactions. A number of hypotheses based on the models of the pairwise complexes and also on the analysis of electrostatic contributions were verified experimentally. Several of the residues predicted from these analyses to be essential for any RING finger-E2 interaction had been previously identified and validated by other laboratories.[23,24] Specifically, the analysis of electrostatic contributions performed with Molaris predicted that all E2 proteins have, at the N-terminus of their RING-finger interaction interface, a pair of basic residues (lysine and arginine) that are essential for their interaction with any RING-finger domains. Additional residues on the E2s are likewise essential for these interactions, the most prominent being K6, R7, K10, and E11 in UBC13 and R5, R6, K9, and E10 in UbcH7, whose relevance has been experimentally demonstrated previously by others.[24] These residues are not predicted to confer interaction selectivity, but to be essential for RING-finger domain-E2 interactions, and the introduction of mutations in these positions by our virtual mutagenesis approach profoundly destabilized the complexes. More expectedly, the analysis of electrostatic contributions with Molaris predicted that the Zn^{2+}-coordinating cysteine and histidine residues are essential for the stability of the RING-finger-E2 complexes. These confirmations represent a validation of our analyses and lend significance to the new predictions made by the present analysis, such as the contribution of the region from residues 95 to 99 of Ubc13 and UbcH7 to the interactions with RING-finger domains. These residues are highly conserved among all E2s, and our observations provide the first evidence that they may be important contributors for the recruitment of any E2 by RING-finger domains.

In summary, the computational approaches used here suggest that the selectivity of recruitment of a given E2 by a particular RING-finger domain resides mainly in specific residues of the RING-finger domains. More specifically, our results suggest that both electrostatic and steric constraints in at least two regions of any RING-finger domain, at either end of its interface with the recruited E2s, determine the selectivity of their interactions with E2s.

METHODS

Yeast two-hybrid screening

Full-length cDNA for human Ubc13 was generated by polymerase chain reaction with specific primers carrying EcoRI and Sal I restriction sites using cDNA from the cell line HepG2 and cloned in frame with the Gal4 DNA-binding domain in pBD (Stratagene, La Jolla, CA). This vector was cotranfected by the lithium acetate method into the *S. cerevisae* strain AH109 together with a human prostate cDNA library cloned in pACT2 (Clontech, Palo Alto, CA). Freshly prepared yeast competent cells were mixed with plasmid together with herring testis carrier DNA and polyethyleneglicol-lithium acetate solution (40% polyethyleneglicol, 10 m*M* Tris, 1 m*M* EDTA, and 100 m*M* lithium acetate) and incubated for 30 min at 30°C with shaking. Seven percent dimethyl sulfoxide was added to the cells and followed by a 42°C heat shock in a water bath. Cells were chilled on ice, centrifuged at 1000*g*, and resuspended in TE buffer (10 m*M* Tris–HCl pH 7.5, 1 m*M* EDTA) before plating in minimal media plates, thus testing for autoactivation of the HIS3, ADE2, and LacZ marker genes contained in the genome of the yeast strain AH109. Shuttle plasmids were isolated from yeast cells grown in minimal media by phenol-chloroform extraction, rescued in *E. coli* and retransformed into AH109 with the bait plasmid. Inserts contained in pACT2 from confirmed interacting positives were analyzed by sequencing by the Sanger method. Screening efficiencies were calculated by plating 1 of 200 of the total transformed yeast on Leu/Trp plates, thus assaying for the incorporation of pBD, which confers triptophan auxotrophy, and pACT2, which confers leucine auxotrophy, and counting the number of independent clones.

Yeast two-hybrid interaction assays

Plasmids pAS2-UbcH7, pAS2-UbcH6, pAS2-cdc34, and pAS2-UBE2E2 were kindly provided by Dr. Ito from Gifu University School of Medicine, Japan, and generated as described.[25] Plasmids pACT2-RNF11 and pACT2-RNF103 and all their mutants were obtained as described in the sections of cloning and site-directed mutagesis, except for pACT2-RNF11, pACT2-ZNFR2, and pACT2-RNF103, that were obtained as positive clones in the

yeast two-hybrid (YTH) screening with Ubc13. The yeast strain and the transformation protocol were the same as in the yeast two-hybrid screening described above (AH109). The YTH assay was performed for each Ubc protein against each RING-finger domain under study.

Molecular modeling

The PFAM database (http://www.sanger.ac.uk) was used to identify all human proteins that contain RING-finger domains, and the Brookhaven Protein Data Bank (PDB) (http://www.pdb.org) to find structural homologs within the RING-finger domain family. Of all the RING-finger proteins with structures deposited in PBD, eight were selected to further determine the best candidates again which to model our proteins.

For those structures that corresponded to protein complexes, only the parameters corresponding to their RING-finger domains were retained. The eight structures were superimposed using Stamp4.2[26] to determine the degree of structural homology among them, using RasMol v2.5,[27] Prepi, and PyMol for their visualization.

Modeller[28] was used to model both RNF11 and RNF103 models using as template the ring finger domain C3HC4 of equine herpes virus-1 (with code 1CHC in the Protein Data Bank) aligned with the Hidden Markov profile of the RING-finger domain generated by the previous structural superimposition with the HMMER package. To analyze the stability of the obtained models, PROSAII[29] was used. The best models obtained after this processing were subjected to Gromos87[30] to minimize their energies. The three best models for each protein were superimposed to the Cbl-UbcH7 structure (PDB: 1FBV) with Stamp, to provide the appropriate position and distance in space between an E2 and an E3 RING finger. The result was visualized with Prepi. The heterodimeric structures were optimized energetically with Gromos87. Structural models of the RING-finger domains in complex with Ubc13 were obtained by superimposing them with the crystal structure of the heterodimer formed by Ubc13 and Mms2 (PDB: 1JAT) with Stamp. The resulting heterodimers were energetically optimized with Gromos87.

Stability analysis

The resulting complexes were analyzed with Molaris[22] in order to evaluate the electrostatic stability of the different residues participating in the modeled interfaces and the contributions from other residues to this stability.[31] This stabilization is evaluated by comparing the solvation energy of each residue in the protein environment to the solvation energy of that residue in solution, by means of the linear response approximation (LRA) version of the semimacroscopic protein dipoles Langevin dipoles (PDLD/S-LRA) method.[32] The methodology has been extensively documented, and only the relevant equations used in this work are shown below. The PDLD/S method evaluates the electrostatic group contribution by averaging the effective potential of transferring a group from solvation to protein,

$$\Delta U^{\mathrm{w}\to\mathrm{p}}_{\mathrm{PDLD/S},i} = \left[\Delta\Delta G^{\mathrm{w}}_{\mathrm{p}}(q_i = 0 \to q_i = \overline{q}_i) - \Delta G^{w}_{q,i}\right] \times \left(\frac{1}{\varepsilon_p} - \frac{1}{\varepsilon_w}\right) - \frac{\Delta V^{p}_{q\mu}(q_i = \overline{q}_i)}{\varepsilon_p} \quad (1)$$

where $\Delta\Delta G^{\mathrm{w}}_{\mathrm{p}}$ represents the change in the microscopic (all-atom) solvation energy of the entire protein plus the group upon changing the charge of this group from zero to its actual charge $\bar{q}_i$, $\Delta G^{w}_{q,i}$ is the solvation energy of the group when it is surrounded just by water molecules (its self energy in water); ε_{p} is the so-called protein dielectric constant (taken as $\varepsilon_{\mathrm{p}} = 4$ in this work); ε_{w} is the water dielectric constant ($\varepsilon_{\mathrm{w}} = 80$); and $\Delta V^{\mathrm{p}}_{q\mu}$ is the contribution from the interaction between the protein residual charges (permanent dipoles) and the group that is being considered.

The actual free energy of solvation of the ith group is evaluated by the proper average of Eq. (1) within the LRA framework[32]:

$$\Delta G^{\mathrm{w}\to\mathrm{p}}_{\mathrm{PDLD/S},i} = \frac{1}{2}\left[\left\langle \Delta U^{\mathrm{w}\to\mathrm{p}}_{\mathrm{PDLD/S},i}\right\rangle_{q_i=0} + \left\langle \Delta U^{\mathrm{w}\to\mathrm{p}}_{\mathrm{PDLD/S},i}\right\rangle_{q_i=\bar{q}_i}\right] \quad (2)$$

Molecular dynamics (MD) calculations were performed for all protein and water atoms in a sphere of 20 Å around the center of the residue being considered, while keeping the rest of the protein fixed following the spherical boundary constraint SCAAS protocol[33] with the local reaction field[34] for long-range electrostatic energies. Thus, for each residue considered (see below) and after 5-ps initial relaxation (with 1 fs stepsize), a total 25-ps production runs were conducted following the above protocol. For every 5 ps, a snapshot of the system was used to evaluate the first term in the right hand side of Eq. (1), getting a final average of five calculations per each residue stability. With this definition of the salvation-free energy of a residue in hand, a series of protocols were introduced to check several aspects of the interface. To start with, only the I residues participating in each interaction interface (within a 10 Å of the partner protein) were selected. Then, the global stability of a protein interface can be qualitatively estimated as $S = \sum_i^I \Delta G^{\mathrm{w}\to\mathrm{p}}_{\mathrm{PDLD/S},i}$. Note that this summatory does not give a quantitative measure of the global stability but an indication of the trend. Finally, we evaluated the S value of the protein of interest (as evaluated by summing up all the residue stabilities) for a series of systems for which the charge of a given residue in the interface region was set to zero. With this "charge zeroing" protocol, we

estimate the electrostatic contributions in a simplified computational alanine scanning protocol, in which we take profit of the conservation of the structure around the residue being considered to efficiently scan a large portion of the protein sequence.

Site-directed mutagenesis

For site-directed mutagenesis, the Quick Change procedure (Stratagene) was used. In a first step, the plasmid of interest was synthesized by the high-fidelity polymerase Pfu with ~30-base pair-complementary oligonucleotides carrying the desired mutation at the center of the sequences. Second, the plasmid template was subjected to Dpn I (Biolabs, UK) digestion for 1 h. Only plasmids of bacterial origin were restricted because Dpn I only cut at methylated sites. After digestion, plasmids were transformed by heat shock (see above) into competent DH5α bacterial cells (Stratagene). Plasmids were isolated and sequenced to confirm the incorporation of the desired mutation.

ACKNOWLEDGMENTS

The authors thankfully acknowledge the computer resources, technical expertise and assistance provided by the Barcelona Supercomputing Center-Centro Nacional de Supercomputación. J. S. was a recipient of a FPI fellowship from the Ministerio de Educación y Ciencia.

REFERENCES

1. Castagnoli L, Costantini A, Dall'Armi C, Gonfloni S, Montecchi-Palazzi L, Panni S, Paoluzi S, Santonico E, Cesareni G. Selectivity and promiscuity in the interaction network mediated by protein recognition modules. FEBS Lett 2004;567:74–79.
2. Nooren IM, Thornton JM. Diversity of protein–protein interactions. EMBO J 2003;22:3486–3492.
3. Basdevant N, Weinstein H, Ceruso M. Thermodynamic basis for promiscuity and selectivity in protein–protein interactions: PDZ domains, a case study. J Am Chem Soc 2006;128:12766–12777.
4. Mayer BJ. SH3 domains: complexity in moderation. J Cell Sci 2001;114(Pt 7):1253–1263.
5. Wiedemann U, Boisguerin P, Leben R, Leitner D, Krause G, Moelling K, Volkmer-Engert R, Oschkinat H. Quantification of PDZ domain specificity, prediction of ligand affinity and rational design of super-binding peptides. J Mol Biol 2004;343:703–718.
6. Durocher D, Henckel J, Fersht AR, Jackson SP. The FHA domain is a modular phosphopeptide recognition motif. Mol Cell 1999;4:387–394.
7. Schleinkofer K, Wiedemann U, Otte L, Wang T, Krause G, Oschkinat H, Wade RC. Comparative structural and energetic analysis of WW domain-peptide interactions. J Mol Biol 2004;344:865–881.
8. Otte L, Wiedemann U, Schlegel B, Pires JR, Beyermann M, Schmieder P, Krause G, Volkmer-Engert R, Schneider-Mergener J, Oschkinat H. WW domain sequence activity relationships identified using ligand recognition propensities of 42 WW domains. Protein Sci 2003;12:491–500.
9. Liu BA, Jablonowski K, Raina M, Arce M, Pawson T, Nash PD. The human and mouse complement of SH2 domain proteins-establishing the boundaries of phosphotyrosine signaling. Mol Cell 2006;22:851–868.
10. Zarrinpar A, Lim WA. Converging on proline: the mechanism of WW domain peptide recognition. Nat Struct Biol 2000;7:611–613.
11. Alam SL, Langelier C, Whitby FG, Koirala S, Robinson H, Hill CP, Sundquist WI. Structural basis for ubiquitin recognition by the human ESCRT-II EAP45 GLUE domain. Nat Struct Mol Biol 2006;13:1029–1030.
12. Jackson PK, Eldridge AG, Freed E, Furstenthal L, Hsu JY, Kaiser BK, Reimann JD. The lore of the RINGs: substrate recognition and catalysis by ubiquitin ligases. Trends Cell Biol 2000;10:429–439.
13. Pickart CM. Mechanisms underlying ubiquitination. Annu Rev Biochem 2001;70:503–533.
14. Ravasi T, Huber T, Zavolan M, Forrest A, Gaasterland T, Grimmond S, Hume DA. Systematic characterization of the zinc-finger-containing proteins in the mouse transcriptome. Genome Res 2003;13(6B):1430–1442.
15. Plans V, Scheper J, Soler M, Loukili N, Okano Y, Thomson TM. The RING finger protein RNF8 recruits UBC13 for lysine 63-based self polyubiquitylation. J Cell Biochem 2006;97:572–582.
16. Christensen DE, Brzovic PS, Klevit RE. E2-BRCA1 RING interactions dictate synthesis of mono- or specific polyubiquitin chain linkages. Nat Struct Mol Biol 2007;14:941–948.
17. Winkler GS, Albert TK, Dominguez C, Legtenberg YI, Boelens R, Timmers HT. An altered-specificity ubiquitin-conjugating enzyme/ubiquitin-protein ligase pair. J Mol Biol 2004;337(1):157–165.
18. Blomberg N, Gabdoulline RR, Nilges M, Wade RC. Classification of protein sequences by homology modeling and quantitative analysis of electrostatic similarity. Proteins 1999;37:379–387.
19. Stiffler MA, Chen JR, Grantcharova VP, Lei Y, Fuchs D, Allen JE, Zaslavskaia LA, Macbeath G. PDZ domain binding selectivity is optimized across the mouse proteome. Science 2007;317:364–369.
20. VanDemark AP, Hofmann RM, Tsui C, Pickart CM, Wolberger C. Molecular insights into polyubiquitin chain assembly: crystal structure of the Mms2/Ubc13 heterodimer. Cell 2001;105:711–720.
21. Zheng N, Wang P, Jeffrey PD, Pavletich NP. Structure of a c-Cbl-UbcH7 complex: RING domain function in ubiquitin-protein ligases. Cell 2000;102:533–539.
22. Lee F, Chu Z-T, Warshel A. Microscopic and semimicroscopic calculations of electrostatic energies in proteins by the POLARIS and ENZYMIX programs. J Comput Chem 1993;14:161–185.
23. Chu ZT, Villà-Freixa J, Strajbl M, Schutz CN, Shurki A, Warshel A. MOLARIS version alpha 9.06.01. 2003.
24. Ulrich HD. Protein–protein interactions within an E2-RING finger complex. Implications for ubiquitin-dependent DNA damage repair. J Biol Chem 2003;278:7051–7058.
25. Ito KAS, Iwakami R, Yasuda H, Muto Y, Seki N, Okano Y. N-Terminally extended human ubiquitin-conjugating enzymes (E2s) mediate the ubiquitination of RING-finger proteins. ARA54 and RNF8. Eur J Biochem 2001;268:2725–2732.
26. Russell RB, Barton GJ. Multiple protein sequence alignment from tertiary structure comparison: assignment of global and residue confidence levels. Proteins 1992;14:309–323.
27. Sayle R. RasMol v2.5. Biomolecular structure, glaxo and development 1994.
28. Sali A, Sánchez R, Badretdinov A. Modeller 1997.
29. Ortner M, Lackner P, Sippl MJ. ProsaII 2001.
30. Scott W. Gromos 1996.
31. Bonet J, Caltabiano G, Khan AK, Johnston MA, Corbi C, Gomez A, Rovira X, Teyra J, Villa-Freixa J. The role of residue stability in transient protein-protein interactions involved in enzymatic phosphate hydrolysis. A computational study. Proteins 2006;63:65–77.
32. Sham YY, Chu ZT, Tao H, Warshel A. Examining methods for calculations of binding free energies: LRA. LIE, PDLD-LRA, and PDLD/S-LRA calculations of ligands binding to an HIV protease. Proteins 2000;39:393–407.
33. Roca M, Messer B, Warshel A. Electrostatic contributions to protein stability and folding energy. FEBS Lett 2007;581:2065–2071.
34. Lee FS, Warshel A. A local reaction field method for fast evaluation of long-range electrostatic interactions in molecular simulations. J Chem Phys 1992;97:3100–3107.